

Supplementary Material

Laser-Assisted Fabrication of Flexible Monofilament Supercapacitor

Phuong Thi Nguyen,¹ Jina Jang,¹ Yoonjae Lee,¹ Seung Tae Choi,² Jung Bin In^{1,3,*}

¹Soft Energy Systems and Laser Applications Laboratory, School of Mechanical Engineering, Chung-Ang University, Seoul, 06974, Republic of Korea

²Functional Materials and Applied Mechanics Laboratory, School of Mechanical Engineering, Chung-Ang University, Seoul, 06974, Republic of Korea

³Department of Intelligent Energy and Industry, Chung-Ang University, Seoul 06974, Republic of Korea

* Corresponding author. E-mail: jbin@cau.ac.kr (J.B. In)

Comparison of laser sintering and hotplate sintering

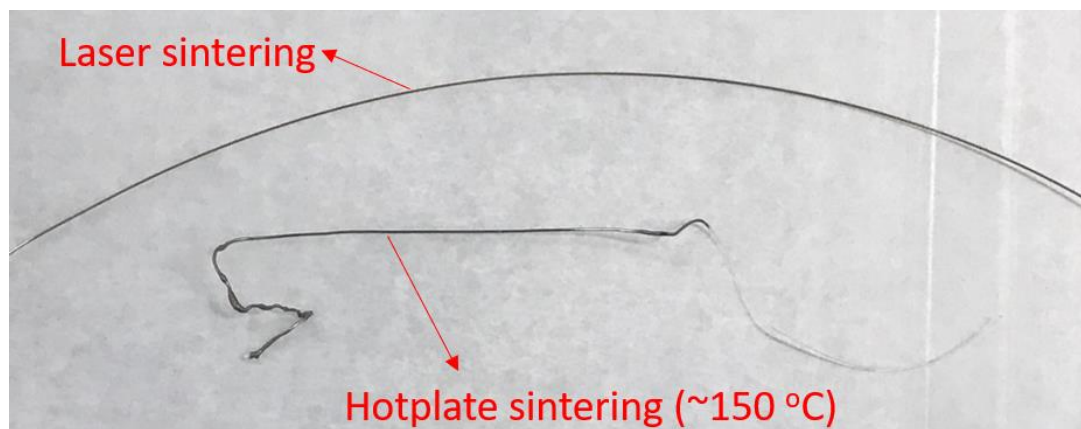


Figure S1. Digital images of AgNP-coated fibers sintered using a 532 nm laser and a hotplate at ~150 °C.

EDS elemental maps of the AgNP/AgNW/Au-coated fiber

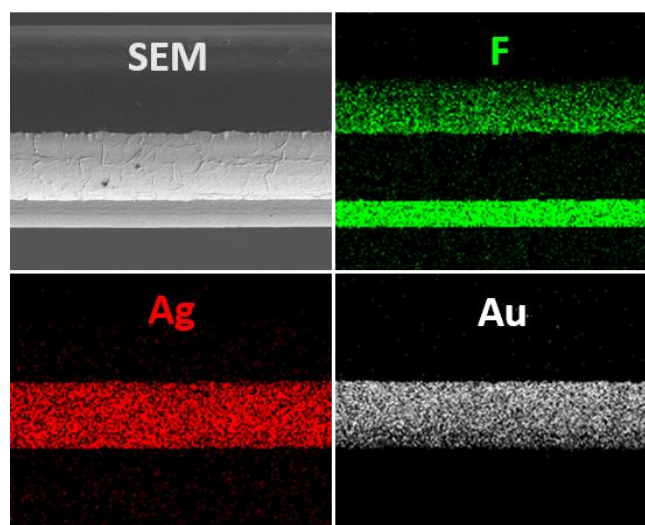


Figure S2. Top-view EDS elemental maps of the AgNP/AgNW/Au-coated fiber.

Comparison of AgNP and AgNP/AgNW layers

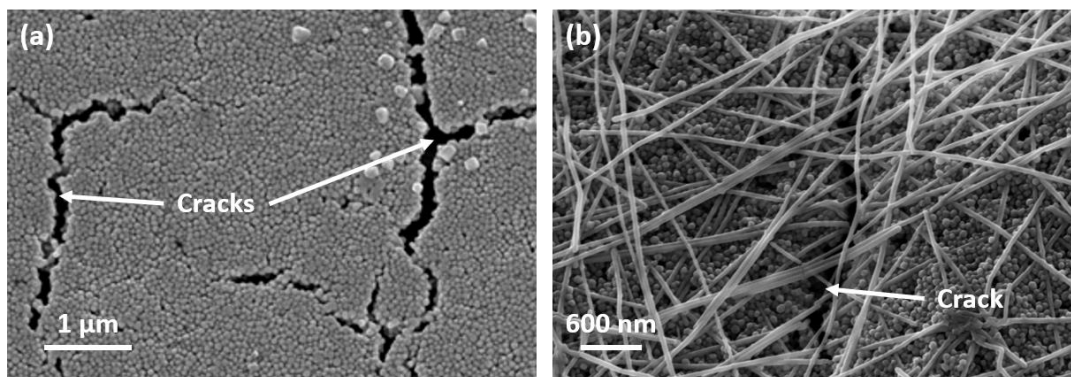


Figure S3. Top-view SEM images of (a) a AgNP layer and (b) a AgNP/AgNW layer near cracks.

Electrochemical characteristics of G-SCs and MG-SCs

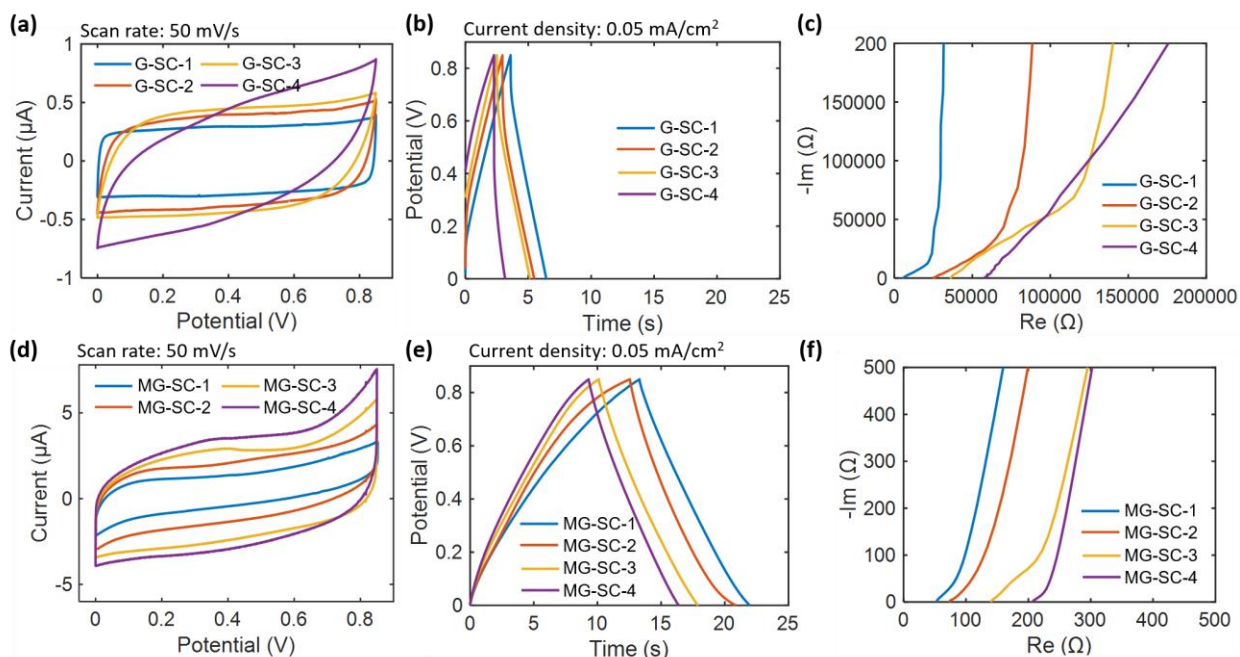


Figure S4. Cyclic voltammetry (CV) , galvanostatic charge/discharge (CC) curve, and electrochemical impedance spectroscopy (EIS) for (a, b, c) G-SCs and (c, d, e) MG-SCs, respectively.

EDX and XPS of MnO₂

Figure S5a shows the energy-dispersive X-ray spectroscopy (EDX; Emax Energy EX-250, Horiba) result of an MGM fiber electrode. The EDX spectrum confirms the existence of Mn and O in the electrode. Figure S5b shows the X-ray photoelectron spectroscopy (XPS; K-alpha Plus, Thermo Fisher Scientific) spectrum collected by the survey scan of a MnO₂ layer that was prepared on a large-area graphene film by using the same electrodeposition method. Figure S5c shows the XPS spectrum of Mn 2p that displays a peak separation of 11.6 eV.

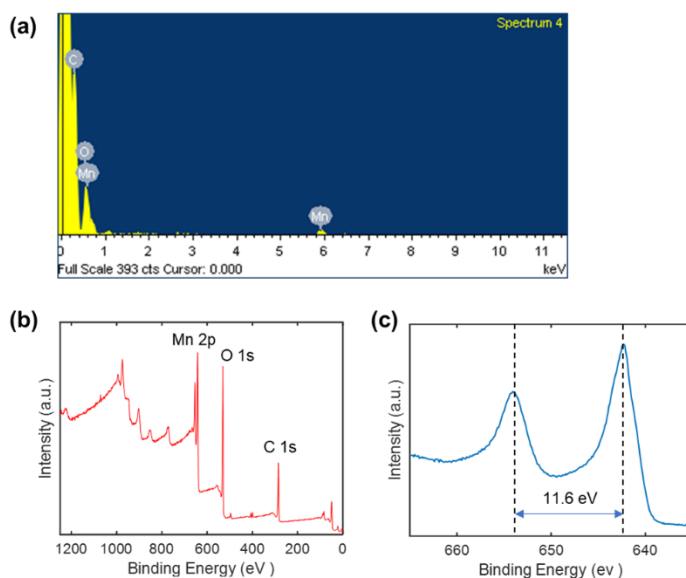


Figure S5. (a) EDX spectrum of an MGM electrode fiber. (b) Survey XPS spectrum and (c) XPS spectrum of Mn 2p that were obtained from a MnO₂ layer that was electrodeposited on a graphene film.

Electrochemical characteristics of MGM-SC obtained via 3-electrode measurements

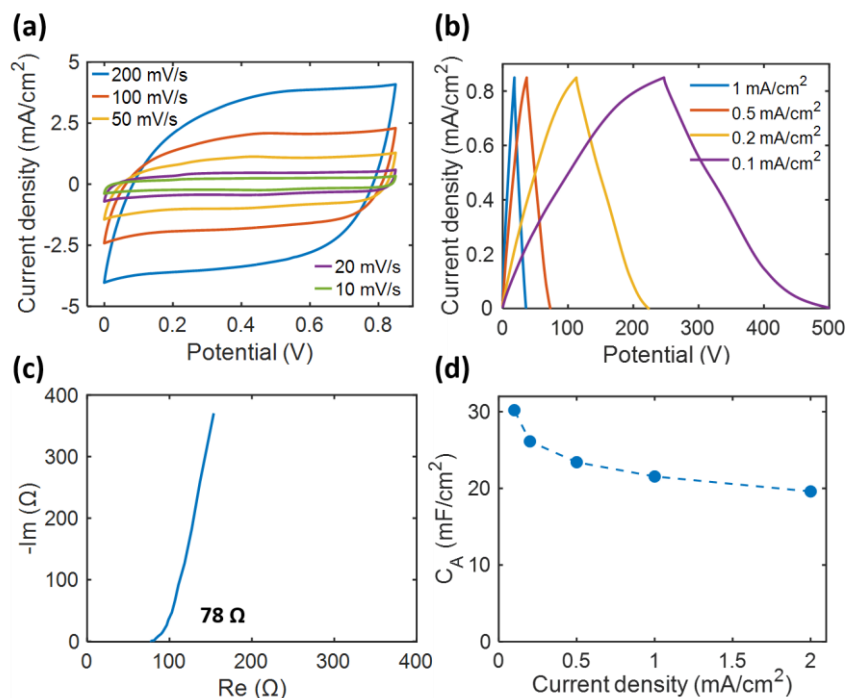


Figure S6. (a) CV , (b) CC , (c) EIS , and (d) areal capacitances at a range of current densities for a single MGM fiber (length: 3.5 cm).

Cyclic charge/discharge testing for MGM-SC

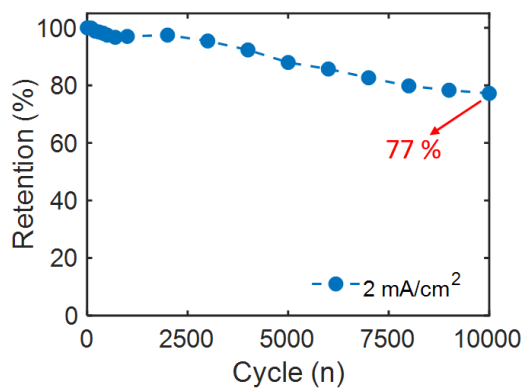


Figure S7. Capacitance retention for 10000 cycles of charge/discharge for MGM-SC.

Ragone plot

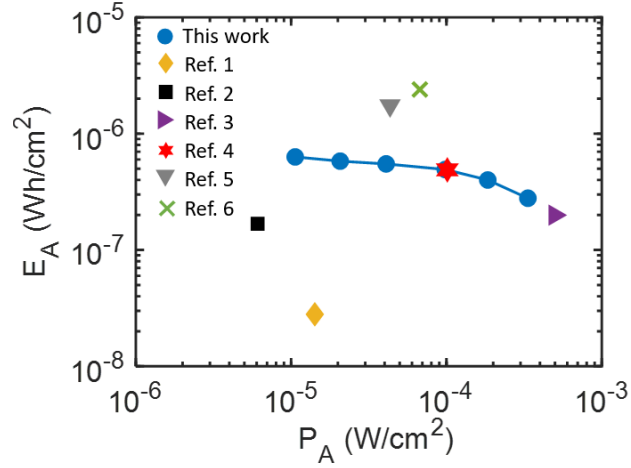


Figure S8. Area-specific Ragone plot of the MGM-SC and other reported fiber SCs. For comparison the data from ref. 1, 2, 3, 4, 5, 6 were reproduced by using Origin® software.

The areal energy density (E_A) and power density (P_A) in this work and ref. 4 and 6 were calculated by:

$$C_{cell} = \frac{I \times t}{(V - IR_{drop})} \quad (F) \quad (1)$$

$$E_A = \frac{1}{2} \times \frac{C_{cell}}{2A} \times \frac{V^2}{3600} \quad (Wh/cm^2) \quad (2)$$

$$P_A = \frac{E_A \times 3600}{t} \quad (W/cm^2) \quad (3)$$

, where I is the discharge current (A), t is the discharge time (s), V is the operation voltage (V), IR_{drop} is the voltage drop at the beginning of the discharge curve (V), and A is the surface area of a single fiber electrode (cm²).^{7, 8} It should be noted that for ref. 2, the C_A and E_A values were calculated by

$$C_A = \frac{I}{A} \times \frac{t}{(V - IR_{drop})} \quad (4)$$

$$E_A = \frac{1}{2} \times C_A \times \frac{V^2}{3600} \quad (5)$$

Stress-strain curve of the PVDF fiber

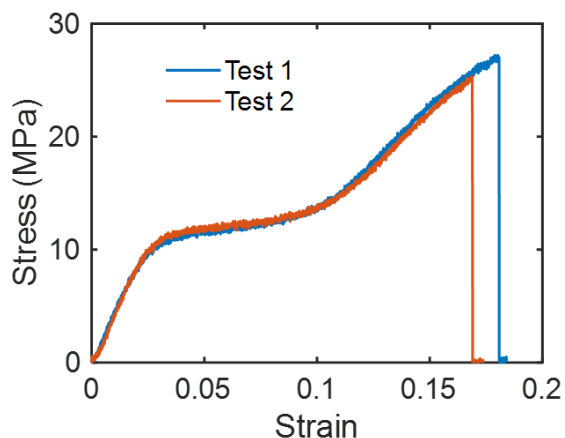


Figure S9. Stress-strain curve of the PVDF fiber.

Droplet-coating method

The AgNPs/AgNWs coated fiber was prepared by using the droplet-coating method. A Ag ink droplet, which was suspended to the syringe needle end, wetted part of the PVDF fiber, enveloping its entire cross-section. The syringe was then translated at a speed of 5 mm/s using a motorized linear stage, so that the droplet swept the entire surface of the fiber. This sweeping was repeated 10 times.

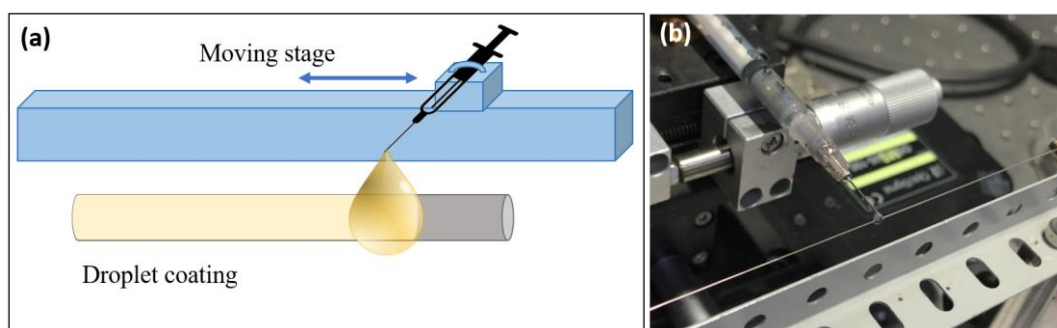


Figure S10. (a) Schematic of the droplet-coating method. (b) Digital image of the droplet-coating setup.

Bendability comparison

Table S1. Bendability comparison of fiber SCs.

Type	Material	Diameter (μm)	Bending angle ($^\circ$)	Bending radius (cm)	Bending times (n)	Retention (%)	ref
All-in-one Monofilament	PVDF fiber, thin metal layer, Gr, MnO_2	SC device fiber: 320–340	180	1.5–0.25	-	92.5	This work
			150	0.75	3000	94	
	GO fiber, rGO	SC device fiber: 50	-	0.75	160	~80	9
Parallel	Au coated polymer fiber + ink	Single electrode fiber: 200	180, 360	-	-	95	10
	Gr based functional fiber	Single electrode fiber: ~50	0–180	-	-	120	8
			180	-	1000	90	
	Cu wire /rGO/ MnO_2	Single electrode fiber: 150	60	-	5000	80	11
	CNT fiber/CNTs/ PANI	Single electrode fiber: 55	0–180	-	-	95	12
			180	-	500	99.8	
	rGO on Au wire	Single electrode fiber: 130	0-120, S shape	-	-	99	13
			90	-	1000	90	
	Hollow Gr/ conducting polymer fiber	Single electrode fiber: 112	0–180	-	-	105	14
			180	-	500	95	
MnO_2 /porous Ni wire	Single electrode fiber: 300	0-180	-	-	90	15	
All-carbon hybrid fibers	Single electrode fiber: 30	120	-	1000	96	16	
		Single electrode fiber: 236	120	-	1000		89
Twisted	MWCNT/ OMC fiber	Single electrode fiber: 150	180	-	1000	90	5
	rGO fiber	SC device fiber: 500	0–360, intertwined	-	-	90	17
			180	-	1000	90	
	SWCNTs/ PANiNW/gel yarn	Single electrode fiber: ~50	0–180	-	-	95	4
GF@PEDOT	Single electrode fiber: 90	0–250	-	-	90	18	
		180	-	300	80		
Coaxial	GF/Gr sheath	SC device fiber: ~190	180	-	100	92	19

Gr: graphene, GF: graphene fiber, rGO: reduced graphene oxide, CNT: carbon nanotube, PANI: polyaniline, MWCNT: multi-walled carbon nanotube, SWCNT: single-walled carbon nanotube, PaniNW: polyaniline nanowires, OMC: ordered mesoporous carbon, PEDOT: Poly(3,4-ethylenedioxythiophene).

Specific capacitance comparison

Table S2. Comparison of specific capacitances of fiber SCs.

Type	Material	Electrolyte	C _L (mF/cm)	C _A (mF/cm ²)	Ref
Monofilament	PVDF fiber, Ag/Au/Gr/MnO ₂	PVA-Na ₂ SO ₄	0.51 at 0.1 mA/cm ²	12.3 at 0.1 mA/cm ² * 9.5 at 2 mA/cm ² *	This work
	GO fiber, rGO	BMIMBF ₄	-	1.2 at 80 μA/cm ²	9
		0.1 M NaClO ₄ in CH ₃ CN	-	0.24 at 200 μA/cm ²	
Parallel	Gr based functional fiber	PVA-H ₂ SO ₄	-	74.25 at 40 mV/s *	8
	Cu/rGO/MnO ₂	PVA-KOH	-	140 at 0.1 mA/cm ²	11
	CNT fiber/CNT/PANI	PVA-H ₃ PO ₄	-	67.31 at 0.5 mA/cm ²	12
	MnO ₂ /porous Ni wire	PVA-KOH	-	847.22 at 0.41 mA/cm ²	15
Twisted	GF/MnO ₂	PVA-H ₂ SO ₄	0.143 at 100 mV/s	9.1–9.6 at 2 μA	20
	Gr/conducting polymer microfibers	PVA-H ₂ SO ₄	0.58 at 0.53 mA/cm ²	15.39 at 0.53 mA/cm ²	18
	SWCNTs/ PAniNW/gel yarn	PVA-H ₂ SO ₄	-	3.065 at 0.2 A/g *	4
Coaxial	Stainless steel, ink, AC	PVA-H ₃ PO ₄	0.1 at 40 μA	3.18 40 μA	21
	Nanoporous Au wire, MnO ₂	PVA-LiCl	-	12 at 0.3 mA/cm ² 6 at 2 mA/cm ²	22

Gr: graphene, GF: graphene fiber, GO: graphene oxide, rGO: reduced graphene oxide, CNT: carbon nanotube, SWCNT: single-walled carbon nanotube, PaniNW: polyaniline nanowires, NW: nanowire.

* The specific capacitance values reported in this paper, ref. 8 and ref. 4 were calculated from the equation:

$$C_X = 2 \frac{I}{X} \times \frac{t}{(V - IR_{\text{drop}})} \quad (6)$$

, where I is the discharge current (A), t is the discharge time (s), V is the operation voltage (V), and IR_{drop} is the voltage drop at the beginning of the discharge curve (V). X can be the effective surface area (A) or length (L) of a single electrode. However, other studies in the table reported the specific capacitance value from the following equation:

$$C_X = \frac{I}{X} \times \frac{t}{(V - IR_{\text{drop}})} \quad (7)$$

Therefore, the specific capacitance value reported in the marked papers has been divided by a factor of 2 in this table for fair comparison.

References

1. J. Bae, M. K. Song, Y. J. Park, J. M. Kim, M. Liu and Z. L. Wang, *Angew. Chem. Int. Ed. Engl.*, 2011, **50**, 1683-1687.
2. Y. Meng, Y. Zhao, C. Hu, H. Cheng, Y. Hu, Z. Zhang, G. Shi and L. Qu, *Adv. Mater.*, 2013, **25**, 2326-2331.
3. P. Xu, T. Gu, Z. Cao, B. Wei, J. Yu, F. Li, J.-H. Byun, W. Lu, Q. Li and T.-W. Chou, *Advanced Energy Materials*, 2014, **4**.
4. Q. Meng, K. Wang, W. Guo, J. Fang, Z. Wei and X. She, *Small*, 2014, **10**, 3187-3193.
5. J. Ren, W. Bai, G. Guan, Y. Zhang and H. Peng, *Adv. Mater.*, 2013, **25**, 5965-5970.
6. C. Choi, S. H. Kim, H. J. Sim, J. A. Lee, A. Y. Choi, Y. T. Kim, X. Lepro, G. M. Spinks, R. H. Baughman and S. J. Kim, *Sci Rep*, 2015, **5**, 9387.
7. D. Yu, Q. Qian, L. Wei, W. Jiang, K. Goh, J. Wei, J. Zhang and Y. Chen, *Chem Soc Rev*, 2015, **44**, 647-662.
8. N. He, W. Shan, J. Wang, Q. Pan, J. Qu, G. Wang and W. Gao, *J. Mater. Chem. A*, 2019, **7**, 6869-6876.
9. Y. Hu, H. Cheng, F. Zhao, N. Chen, L. Jiang, Z. Feng and L. Qu, *Nanoscale*, 2014, **6**, 6448-6451.
10. Y. Fu, X. Cai, H. Wu, Z. Lv, S. Hou, M. Peng, X. Yu and D. Zou, *Adv. Mater.*, 2012, **24**, 5713-5718.
11. M. Huang, L. Wang, S. Chen, L. Kang, Z. Lei, F. Shi, H. Xu and Z.-H. Liu, *Rsc Adv*, 2017, **7**, 10092-10099.
12. J.-h. Liu, X.-y. Xu, W. Lu, X. Xiong, X. Ouyang, C. Zhao, F. Wang, S.-y. Qin, J.-l. Hong, J.-n. Tang and D.-Z. Chen, *Electrochim. Acta*, 2018, **283**, 366-373.
13. Y. Li, K. Sheng, W. Yuan and G. Shi, *Chem Commun (Camb)*, 2013, **49**, 291-293.
14. G. Qu, J. Cheng, X. Li, D. Yuan, P. Chen, X. Chen, B. Wang and H. Peng, *Adv. Mater.*, 2016, **28**, 3646-3652.
15. P. Li, J. Li, Z. Zhao, Z. Fang, M. Yang, Z. Yuan, Y. Zhang, Q. Zhang, W. Hong, X. Chen and D. Yu, *Adv Sci (Weinh)*, 2017, **4**, 1700003.
16. W. Jiang, S. Zhai, Q. Qian, Y. Yuan, H. E. Karahan, L. Wei, K. Goh, A. K. Ng, J. Wei and Y. Chen, *Energy & Environmental Science*, 2016, **9**, 611-622.
17. N. He, J. Liao, F. Zhao and W. Gao, *ACS Appl Mater Interfaces*, 2020, **12**, 15211-15219.
18. Y. Meng, L. Jin, B. Cai and Z. Wang, *Rsc Adv*, 2017, **7**, 38187-38192.
19. X. Zhao, B. Zheng, T. Huang and C. Gao, *Nanoscale*, 2015, **7**, 9399-9404.
20. Q. Chen, Y. Meng, C. Hu, Y. Zhao, H. Shao, N. Chen and L. Qu, *J. Power Sources*, 2014, **247**, 32-39.
21. D. Harrison, F. Qiu, J. Fyson, Y. Xu, P. Evans and D. Southee, *Phys. Chem. Chem. Phys.*, 2013, **15**, 12215-12219.
22. H. Xu, X. Hu, Y. Sun, H. Yang, X. Liu and Y. Huang, *Nano Research*, 2014, **8**, 1148-1158.